Eur Biophys J (1999) 28: 468–477 

ARTICLE

D. Lazár · P. Pospíšil

# Mathematical simulation of chlorophyll *a* fluorescence rise measured with 3-(3′,4′-dichlorophenyl)-1,1-dimethylurea-treated barley leaves at room and high temperatures

Received: 27 August 1998 / Revised version: 12 March 1999 / Accepted: 8 April 1999

**Abstract** Chlorophyll *a* fluorescence induction (FI) measured by Plant Efficiency Analyser fluorometer at room temperature shows a typical O-J-I-P pattern which is at high temperature changed to an O-K-P pattern with a new step K. It has been suggested that the appearance of the K step reflects inhibition of an oxygen evolving complex (OEC). When FI is measured at room temperature with the photosystem II (PSII) herbicide 3-(3′,4′-dichlorophenyl)-1,1-dimethylurea (DCMU), which blocks electron transport from $Q_A$ to $Q_B$ (the first and the second quinone electron acceptors in PSII, respectively), the time course of the FI shows a sigmoidal increase to the maximal fluorescence which is reached at a little longer time than that of the J step. Similarly, the FI measured at high temperature with DCMU reaches the maximal value of fluorescence at the time which is a little longer than that of the K step. On the other hand, the reversible radical pair model (RRP) describes energy utilization and electron transport up to $Q_A$. In this work we present the first, to our knowledge, RRP model extended by a description of the function of the donor side of PSII. Assuming the inhibition of the OEC or its full function, the extended RRP model successfully simulates the fluorescence rise measured with DCMU at high and room temperatures, respectively. The roles of the initial state of the OEC and the values of the rate constants in the extended RRP on the simulations of the fluorescence rise at room and high temperatures are also discussed.

**Key words** High temperature stress · Chlorophyll *a* · Fluorescence induction · Reversible radical pair model · Oxygen evolving complex

D. Lazár (✉) · P. Pospíšil
Department of Experimental Physics,
Faculty of Science, Palacký University, tř. Svobody 26,
CZ-771 46 Olomouc, Czech Republic
e-mail: lazard@risc.upol.cz

## Introduction

Since 1931, when Kautsky and Hirsch (1931) published the first scientific article on chlorophyll *a* fluorescence induction (FI), the method has found widespread use in photosynthesis research. This is because it is quickly measured, is not destructive, and the fluorescence signal contains important information about the photosynthetic apparatus (see Krause and Weis 1991; Govindjee 1995). In 1991–92, results of measurements of FI using a Plant Efficiency Analyser (PEA) fluorometer were introduced by Strasser and Govindjee (1991, 1992). Using red LED diodes for an excitation, the PEA allows measurements of FI from 10 μs after onset of excitation light. A typical curve of FI measured by a PEA is characterized by an O-J-I-P pattern, with the J, I, and P steps appearing at about 2, 20, and 200 ms, respectively (see Strasser and Govindjee 1991, 1992; Strasser et al. 1995). However, note that the particular steps are clearly visible only on a logarithm time-axis.

As fluorescence is mainly emitted by photosystem II (PSII) at room temperature (see Krause and Weis 1991; Dau 1994), the O-J-I-P pattern of FI also reflects the state of PSII. The O step (O for origin) corresponds to minimal fluorescence $F_0$ (also called initial fluorescence) which is obtained when all functional reaction centres of PSII (RCII) are open (see Krause and Weis 1991). $F_0$ is not zero because it is an expression of the excitation energy transfer equilibrium in the light harvesting complexes (see Owens 1996) as derived by Laible et al. (1994). In reality, the measured $F_0$ also includes photosystem I fluorescence (Pfündel 1998). There is experimental and theoretical evidence that the O-J phase is the "photochemical phase" connected with primary photochemistry, i.e. reduction of the primary electron acceptor in PSII, pheophytin, and the first quinone electron acceptor of PSII, $Q_A$ (Delosme 1967; Neubauer and Schreiber 1987; Strasser and Govindjee 1991, 1992; Stirbet and Strasser 1995; Stirbet et al. 1995, 1998; Strasser et al. 1995; Lazár et al. 1997a, 1998). On the

other hand, the J-I-P rise is the "thermal phase" (Delosme 1967; Neubauer and Schreiber 1987), reflecting subsequent accumulation of singly or doubly reduced $Q_B$ (the second quinone electron acceptor of PSII) (Strasser and Govindjee 1991, 1992; Stirbet and Strasser 1995; Stirbet et al. 1995, 1998; Strasser et al. 1995; Lazár et al. 1997a). Heterogeneity in reduction of the plastoquinone pool (Strasser et al. 1995; Barthélemy et al. 1997) has also been suggested to be reflected in the J-I-P rise. The I step has also been found to reflect organization of the light harvesting complexes (Barthélemy et al. 1997). Further, Strasser et al. (1995) have established that there is an equivalence of the J step with an $I_1$ step and the I step with an $I_2$ step, the $I_1$ and $I_2$ being intermediate steps of FI measured using extremely high light irradiation (Neubauer and Schreiber 1987). Owing to this equivalence, the J-I rise should be affected by the state of the oxygen evolving complex (OEC), as was found for the $I_1$-$I_2$ rise by Schreiber and Neubauer (1987). For further information on FI in general see a recent review by Lazár (1999).

After high temperature stress of plant material (47 °C for 5 min, or by linear heating up to this temperature), a new step K at about 300 μs appears in the FI (Guissé et al. 1995a, b; Lazár and Ilík 1997; Lazár et al. 1997b; Srivastava et al. 1997; Strasser 1997). It has been suggested that the appearance of the K step is caused by the inhibition of the OEC (Guissé et al. 1995a, b; Srivastava et al. 1997; Strasser 1997), but the appearance of the K step also reflects changes in the organization of the light harvesting complexes of PSII (Srivastava et al. 1997). When the PSII herbicide 3-(3′,4′-dichlorophenyl)-1,1-dimethylurea (DCMU) is applied, which blocks electron transport from $Q_A$ to $Q_B$ by binding to the $Q_B$ site of the D1 protein of PSII (Oettmeier and Soll 1983; Trebst and Draber 1986; Trebst 1987; Shigematsu et al. 1989), only the primary photochemistry can occur and $Q_A^-$ accumulates. This leads, in the case of FI measured at room temperature, to a sharp rise of fluorescence which reaches its maximum at (or near) the position of the J step (see Guissé et al. 1995a, b; Strasser et al. 1995; Lazár et al. 1997a, 1998; Srivastava et al. 1997). On the other hand, when DCMU is applied and the plants are stressed by the high temperature, fluorescence rises sharply again but now it reaches maximal value at (or near) the position of the K step (Guissé et al. 1995a, b; Srivastava et al. 1997).

Excitation energy utilization and photochemical reactions in RCII can be very well described by the reversible radical pair (RRP) model, also called the exciton radical pair equilibrium model first proposed by Breton (1983) (see also van Grondelle 1985; Schatz et al. 1988; Dau 1994). Even if the O-J-I-P transient has been mainly simulated on the basis of electron transport between $Q_A$ and $Q_B$ (Stirbet and Strasser 1995; Stirbet et al. 1995, 1998; Lazár et al. 1997a), the RRP model has also been used for a simulation or a fitting of the time course of FI (Baake and Schlöder 1992; Trissl et al. 1993; Lavergne and Trissl 1995; Trissl and Lavergne 1995; Vavilin et al. 1998), but not FI measured by a PEA fluorometer.

In this work, based on the RRP model extended by a description of the function of the donor side of PSII, and assuming a full function or an inhibition of the OEC, we present simulations of the fluorescence rise measured with DCMU at both room and high temperatures. The simulations agree well with the experimental results. The roles of other parameters in the extended RRP model are also discussed.

## Materials and methods

Chlorophyll *a* fluorescence induction curves were measured with the primary leaves of nine-day-old spring barley (*Hordeum vulgare* cv. Akcent). The plants were grown at 25 °C in a growth chamber (85% humidity) on artificial soil composed of Perlite and supplied with Knopp solution. The light/dark regime was 16 h light/8 h dark with continuous white irradiation (90 μmol $m^{-2}$ $s^{-1}$), obtained from Philips SL-Prismatic bulbs (25 W). The concentration of chlorophyll ($a$ + $b$) in the leaves was determined according to the method of Lichtenthaler (1987) and it was about 14 μg $cm^{-2}$. A 1 cm long tip of the leaf blade was detached, and the following 2 cm long leaf segment was used for measurements of FI from the adaxial side of the leaf segment.

For room temperature measurement, FI was measured at 25 °C after 30 min of dark adaptation of the leaf. Measurements of FI that had the K step were taken after 30 min of dark adaptation, followed by 5 min of dark immersion of the leaf in a distilled water bath at 47 °C. Measurements of FI with the PSII herbicide DCMU (Sigma, Deisenhofen, Germany) were performed in the same way as described above, but after 2 h dark incubation of leaves in 200 μM DCMU solution. DCMU was dissolved in ethanol and then added to distilled water in such a way that the ethanol was 1/100th of the final volume of the DCMU solution. The low concentration of ethanol was chosen to avoid possible inhibition of electron transport by ethanol (Masamoto and Nishimura 1978). Chlorophyll *a* FI measurements were made with a PEA fluorometer (Hansatech, Norfolk, UK) with irradiation of about 3400 μmol $m^{-2}$ $s^{-1}$ of red light ($\lambda_{max}$ 650 nm). The irradiation was measured with a quantum radiometer LI-189 (LI-COR, Lincoln, USA).

## Theory

### Description of the RRP model

A scheme of the extended RRP model is shown in Fig. 1. This model describes energy utilization and electron transport from P680 to $Q_A$, but also a reduction of $P680^+$ by the donor side of PSII. The reactions are as-

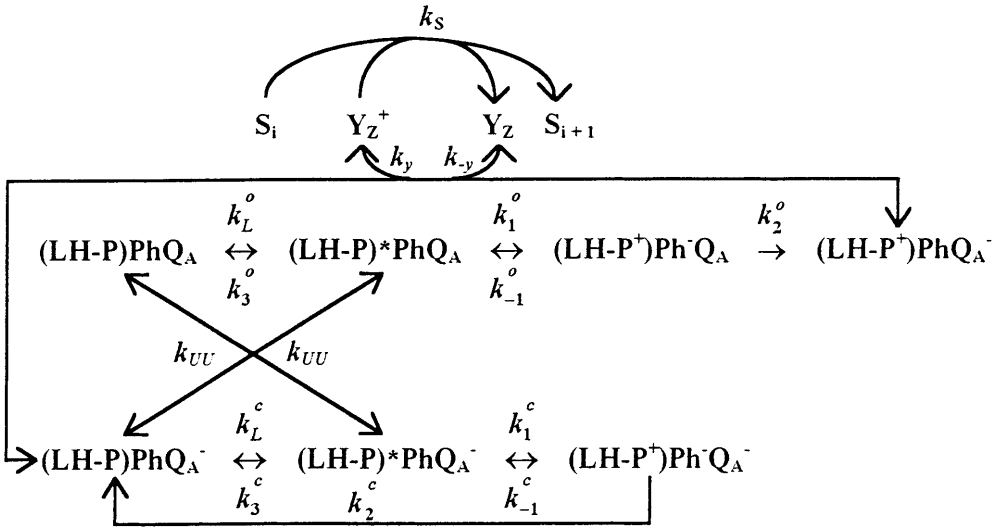


**Fig. 1** A scheme of the extended reversible radical pair model. *LH* denotes light harvesting antenna complexes of photosystem II, *P* and *Ph* denote P680 and pheophytin, respectively. $Y_Z$ is the donor of electrons (tyrosine 161) to $P680^+$ whereas $S_i$ and $S_{i+1}$ are particular states of the oxygen evolving complex (OEC). *Superscripts* – and + denote reduced or oxidized forms, respectively, whereas *superscript* * denotes an excited state. $k_y$ and $k_{-y}$ are forward and backward rate constants for the reduction of $P680^+$ by $Y_Z$, whereas $k_S$ is the rate constant for the transition of the OEC from the $S_i$ state to the $S_{i+1}$ state. $k_1^0$, $k_{-1}^0$, $k_2^0$ are the rate constants for the charge separation, recombination, and stabilization, respectively, in the open reaction centres of photosystem II (RCII). The rate constants for the charge separation and recombination in the closed RCII are denoted as $k_1^c$ and $k_{-1}^c$, respectively, and $k_2^c$ denotes nonradiative charge recombination in the closed RCII to the ground state. Energy transfer between the closed and the open RCIIs is expressed by the rate constant $k_{UU}$. For the rate constants of the deactivation of excited states through heat dissipation or emission as fluorescence in the open ($k_3^0$) and the closed RCIIs ($k_3^c$), we assume that $k_3^0 = k_3^c = k_3$. The equality we also assume for the rates of exciton formation in light harvesting antenna complexes in the open ($k_L^0$) and the closed RCIIs ($k_L^c$) expressed by $k_L^0 = k_L^c = k_L^0$. The values of particular rate constants are shown in Table 1, and the initial conditions for the S states of the OEC are described in the text and in Table 2

sumed to be of the first order with respect to one component and they follow the mass action theory.

Three different possibilities of $P680^+$ reduction by the donor side of PSII are considered in our simulations of fluorescence rise at room temperature. A mixture of these possibilities then forms a global way of $P680^+$ reduction (contribution of every possibility of the $P680^+$ reduction to the global way differs in particular simulations). The possibilities are:

First, as is well known, when FI is measured without DCMU at room temperature, there is the J step, and when FI is measured with DCMU at the same temperature, the fluorescence signal reaches its maximal value at (or near) the position of the J step (see Fig. 2). At room temperature, $P680^+$ is reduced by $Y_Z$ (tyrosine 161, the second donor of electrons in PSII) which is, in turn, reduced by the OEC (see reviews by Hansson and Wydrzynski 1990; Debus 1992; Britt 1996). As reduction of $Q_A$ in the extended RRP model needs only one electron (one turnover of the RCII, see e.g. Srivastava et al. 1997), we must not consider all the S state transitions of the OEC, but only the transition from the initially populated S state (dark adapted state) to the subsequent one. If we assume that there is one stable dark adapted state of the OEC, $S_1$ (Messinger and Renger 1993), we shall rewrite the reactions in the extended RRP model by the following set of differential equations, where the symbol $\dot{x}_i$ represents the time derivation of the form on the left of the symbol.

$$\text{(LH-P)PhQ}_\text{A}\text{: } \dot{x}_1 = -x_1(k_\text{L} + x_6 k_\text{UU}) + x_2(k_3 + x_5 k_\text{UU})$$
$$\text{(LH-P)*PhQ}_\text{A}\text{: } \dot{x}_2 = x_1(k_\text{L} + x_6 k_\text{UU}) - x_2(k_1^\text{o} + k_3 + x_5 k_\text{UU}) + x_3 k_{-1}^\text{o}$$
$$\text{(LH-P}^+\text{)Ph}^-\text{Q}_\text{A}\text{: } \dot{x}_3 = x_2 k_1^\text{o} - x_3(k_{-1}^\text{o} + k_2^\text{o})$$
$$\text{(LH-P}^+\text{)PhQ}_\text{A}^-\text{: } \dot{x}_4 = x_3 k_2^\text{o} - x_4 k_y x_8 + x_5 k_{-y} x_9$$

$$\text{(LH-P)PhQ}_\text{A}^-\text{: } \dot{x}_5 = -x_5(k_\text{L} + x_2 k_\text{UU}) + x_6(k_3 + x_1 k_\text{UU}) + x_7 k_2^\text{c} + x_4 k_y x_8 - x_5 k_{-y} x_9$$
$$\text{(LH-P)*PhQ}_\text{A}^-\text{: } \dot{x}_6 = x_5(k_\text{L} + x_2 k_\text{UU}) - x_6(k_1^\text{c} + k_3 + x_1 k_\text{UU}) + x_7 k_{-1}^\text{c}$$
$$\text{(LH-P}^+\text{)Ph}^-\text{Q}_\text{A}^-\text{: } \dot{x}_7 = x_6 k_1^\text{c} - x_7(k_{-1}^\text{c} + k_2^\text{c})$$
$$\text{Y}_\text{Z}\text{: } \dot{x}_8 = -x_4 x_8 k_y + x_5 k_{-y} x_9 + x_9 k_\text{S} x_{10}$$
$$\text{Y}_\text{Z}^+\text{: } \dot{x}_9 = x_4 x_8 k_y - x_5 k_{-y} x_9 - x_9 k_\text{S} x_{10}$$
$$\text{S}_1\text{: } \dot{x}_{10} = -x_9 k_\text{S} x_{10}$$

with initial conditions:

$$x_1(0) = x_8(0) = x_{10}(0) = 1$$

and

$$x_2(0) = x_3(0) = x_4(0) = x_5(0) = x_6(0) = x_7(0) = x_9(0) = 0$$

The fluorescence of this system, $F_{S1}$, is proportional to a deactivation of the excited states through $k_3$ (Baake and Schlöder 1992) as:

$$F_{S1} = k_3(x_2 + x_6)$$

Second, we have also assumed that, in addition to the $S_1$ state, there is another dark adapted state of the OEC, the $S_0$ state [13% of $S_0$ and 87% of $S_1$ (Haumann and Junge 1994) or 25% of $S_0$ and 75% of $S_1$ (Kok et al. 1970)]. The set of differential equations for the initial $S_0$ state is the same as for the initial $S_1$ state as mentioned above, but the set differs in a value of the rate constant describing the particular S state transition of the OEC, $k_S$ (see Table 1). The initial values for $x_2(0) - x_7(0)$ and $x_9(0)$ are zero, but the initial values for $x_1(0)$, $x_8(0)$, and $x_{10}(0)$ depend on the initial, dark adapted state of all the OEC (initially both the $S_1$ and the $S_0$ states) assumed for the particular simulation, and are summarized in Table 2 (see Results for the explanation). The fluorescence of PSII initially with the $S_0$ state is expressed by the same formula as the fluorescence of PSII initially with the $S_1$ state.

Third, we have also assumed the existence of inactive OECs even at room temperature [up to 30% of all OEC (Conjeaud et al. 1979; Schlodder et al. 1984)]. At PSII with the inactive OEC, we assumed that $P680^+$ is reduced by $Y_Z$ which is not, in turn, reduced by the OEC, the same as in the case of the high temperature stressed PSII with inhibited OEC (see below). The set of differential equations describing PSII with the inactive OEC is the same as for the initial $S_1$ (or $S_0$) state, but because there is no S state transition of the OEC (thus $k_S = 0$), the rightmost products in $\dot{x}_8$ and $\dot{x}_9$ are missing. Because of the same reason, the expression for $\dot{x}_{10}$ is missing too. Further, there is a decrease of values of the rate constants $k_y$ and $k_{-y}$ at PSIIs with the inactive OEC (Conjeaud et al. 1979; Schlodder et al. 1984; Reifarth et al. 1997; see Table 1). The initial values of $x_2(0) - x_7(0)$ and $x_9(0)$ are zero, but the initial values of $x_1(0)$ and $x_8(0)$ depend on the initial, dark adapted state of all the OEC (initially inactive OEC and active OEC at both the $S_1$ and the $S_0$ states) assumed for the particular simulation, and are summarized in Table 2 (see Results for the explanation). The fluorescence of PSII with the inactive OEC is expressed by the same formula as the fluorescence of PSII initially with the $S_1$ state.

On the other hand, when FI is measured without DCMU at high temperature, the K step appears in FI, and when FI is measured with DCMU at the same temperature, the fluorescence signal reaches its maximal value at (or near) the position of the K step (see Fig. 2). As the appearance of the K step reflects the inhibition of the OEC (see Introduction), we have assumed the same for FI measured with DCMU at high temperature. The origin of the K step in the inhibition of the OEC is also in agreement with the results of Cramer et al. (1981) and Thompson et al. (1986), who found a denaturation temperature of the OEC to be about 44–48 °C, which includes the temperature of the K step appearance (about 47 °C). Thus, as mentioned above for the inactive OEC, at the temperature when the K step appears, $P680^+$ is reduced by $Y_Z$ which is not, in turn, reduced by the OEC (see Strasser 1997). It leads to the same set of differential equations as mentioned above for the inactive OEC. The initial conditions are as follows

**Table 1** Values of the rate constants (in $s^{-1}$) at the extended RRP model used in the simulations. For the meaning of particular rate constants, see Fig. 1. The derivation of $k_L$ is presented in the theory section

| Rate constants[a] | Fluorescence rise at room temperature | | | Fluorescence rise at high temperature |
|---|---|---|---|---|
| | Functioning OEC | | Inactive OEC | Inhibited OEC |
| | At the $S_1$ state | At the $S_0$ state | | |
| $k_S$ [A] | 10000 | 5000 | 0 | 0 |
| $k_y$ [B, C, D, E] | $2.9 \times 10^7$ | | $2 \times 10^5$ | $2 \times 10^5$ |
| $k_{-y}$ [B, C, D, E] | $5.8 \times 10^6$ | | $4 \times 10^4$ | $4 \times 10^4$ |
| $k_1^o$ [F, G] | | $9.3 \times 10^9$ | | $6.3 \times 10^9$ |
| $k_2^o$ [F, G] | | $1 \times 10^9$ | | $2.2 \times 10^9$ |
| $k_1^o$ [F, G] | | $3 \times 10^9$ | | $1.5 \times 10^9$ |
| $k_1^c$ [F, G] | | $1.2 \times 10^9$ | | $1 \times 10^9$ |
| $k_{-1}^c$ [F, G] | | $3 \times 10^9$ | | $5 \times 10^9$ |
| $k_{-2}^c$ [F, G] | | $2.5 \times 10^8$ | | $1.5 \times 10^8$ |
| $k_3$ [G] | | $5 \times 10^8$ | | |
| $k_{UU}$ [H, I] | | $1 \times 10^9$ | | |
| $k_L$ | | 5500 | | |

[a] A, see Rappaport et al. (1994); B, Conjeaud et al. (1979), C, Brettel et al. (1984); D, Schlodder et al. (1984); E, Reifarth et al. (1997); F, Schatz et al. (1988); G, Briantais et al. (1996); H, Lavergne and Trissl (1995); I, Trissl and Lavergne (1995)

**Table 2** The initial values for $x_1(0)$ and $x_8(0)$ used in the simulations for the inactive OEC, and for $x_1(0)$, $x_8(0)$, and $x_{10}(0)$ used in the simulations for the active OEC, initially both at the $S_1$ and $S_0$ states

| The OEC | Figure 5 | | | Figure 6 | | |
|---|---|---|---|---|---|---|
| | Curve b | Curve c | Curve d | Curve b | Curve c | Curve d |
| At the $S_1$ state | 1 | 0.87 | 0.75 | 0.7 | 0.61 | 0.53 |
| At the $S_0$ state | 0 | 0.13 | 0.25 | 0 | 0.09 | 0.17 |
| Inactive | 0 | 0 | 0 | 0.3 | 0.3 | 0.3 |

$$x_1(0) = x_8(0) = 1$$

and

$$x_2(0) = x_3(0) = x_4(0) = x_5(0) = x_6(0) = x_7(0) = x_9(0) = 0$$

As Tris treatment results in the inhibition of the OEC (see e.g. Debus 1992), we used the values of the rate constants $k_y$ and $k_{-y}$ found for Tris treated samples (Conjeaud et al. 1979; Reifarth et al. 1997) which are, of course, the same as those ones used for the inactive OEC (see Table 1). The fluorescence of PSII with the inhibited OEC is expressed by the same formula as the fluorescence of PSII initially with the $S_1$ state.

We have not considered the possible quenching of the fluorescence by the $P680^+$ molecule itself (Butler 1972; Sonneveld et al. 1979; Shinkarev and Govindjee 1993) in the extended RRP model; however, we have tested if an omission of this quenching plays any significant role or not. Using another version of the extended RRP model which includes quenching of the excited state by the $P680^+$ molecule itself (with time constant of 1 ns; see Trissl et al. 1993; Bruce et al. 1997), we have obtained a simulated curve (for fluorescence rise with DCMU at high temperature) which only differs in the maximal value of fluorescence by about 2.9% (data not shown). This result implies that the quenching of the fluorescence signal by the $P680^+$ molecule itself does not play any significant role in FI experiments, as has already been stated by Lavergne and Trissl (1995).

The simulations of the fluorescence rise were performed numerically by a program called Scientist (MicroMath, Salt Lake City, USA) using a sophisticated method Episode for stiff systems. Besides the set of differential equations, and the initial conditions (Table 2), values of the rate constants used in the simulations were those summarized in Table 1.

### Derivation of the rate of exciton formation in the antennae complexes ($k_L^o$, $k_L^c$)

All values of the rate constants used in the simulations were those already available in the literature, except for the rate of exciton formation $k_L$ which depends on the experimental conditions. After correcting for the applied excitation light irradiation of 3400 μmol photons $m^{-2}$ $s^{-1}$ to the illuminated leaf area, we obtain $4.27 \times 10^{-2}$ μmol photons $s^{-1}$. After correction for the chlorophyll ($a$ + $b$) concentration in the leaves (14 μg $cm^{-2}$) to the illuminated leaf area, and considering average molecular weight of chlorophyll ($a$ + $b$) to be 900.5 g $mol^{-1}$, we obtain $1.95 \times 10^{-3}$ μmol chlorophyll ($a$ + $b$). Dividing the amount of photons $s^{-1}$ by the amount of chlorophyll ($a$ + $b$) ($4.27 \times 10^{-2}$/ $1.95 \times 10^{-3}$), we obtain a value of ≈22 photons $s^{-1}$ (chlorophyll molecule)$^{-1}$. Then, assuming 250 chlorophyll ($a$ + $b$) in one PSII of barley (see Melis 1996), we obtain 5500 photons $s^{-1}$. This number is the value used in the simulations for the rate of exciton formation for open and closed RCII: $k_L^o = k_L^c = 5500\,s^{-1} = k_L$.

## Results

### Experimental curves

Time courses of typical FIs measured with barley leaves at room (25 °C) and high (47 °C, 5 min) temperatures are shown in Fig. 2 (curves a and b, respectively). The initial rise of fluorescence to the K steps occurs in the case of the high temperature stressed leaves in shorter time than the rise of fluorescence to the J step in an unstressed barley leaf. At room temperature, and to some extent also at higher temperature, the curves a and b reflect electron transport through all PSII, i.e. not only to $Q_A$, as is described by the extended RRP model, but also to $Q_B$ and the plastoquinone pool. The later electron transport is reflected in the J-I-P (K-P) transition (see Stirbet and Strasser 1995; Stirbet et al. 1995, 1998; Strasser et al. 1995; Lazár et al. 1997a). However, when the FI is measured with the PSII herbicide DCMU, which blocks electron transport from $Q_A$ to $Q_B$, we obtain the same system as is described by the extended RRP model. The curves of FI measured with DCMU with barley leaves at room (25 °C) and high (47 °C, 5 min) temperatures are also shown in Fig. 2 (curves c and d, respectively). The curves c and d show that the maximal levels of the fluorescence intensities are reached at little longer times than the J and K steps, respectively. Nevertheless, a shift of the position of the maximal value of the fluorescence intensity measured at high temperature to shorter time in comparison with that one measured at room temperature, both DCMU treated, is

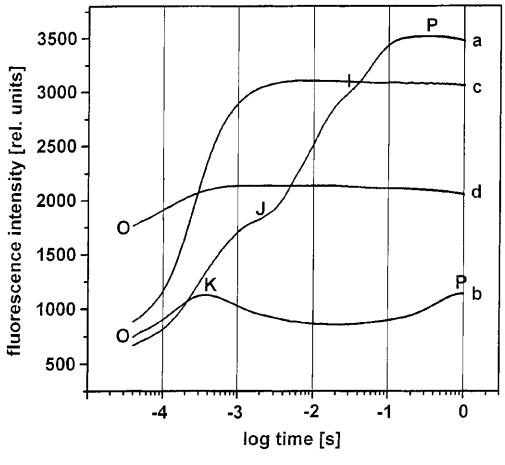


**Fig. 2** Chlorophyll *a* fluorescence induction of barely leaves measured by a PEA fluorometer at room (25 °C, curve *a*) and high temperatures (47 °C for 5 min, curve *b*), and measured at room temperature after DCMU treatment (curve *c*), and measured at the high temperature after DCMU treatment at room temperature (curve *d*). The *O*, *K*, *J*, *I* and *P* steps are labelled

evident. It is the same as the shift of the K step to shorter time in comparison with the J steps in DCMU untreated barley leaves. Very similar results have also been found by Guissé et al. (1995a, b) and Srivastava et al. (1997).

## Basic simulations

At the temperature when the K step appears in FI, the OEC should be completely inhibited and $P680^+$ is reduced by $Y_Z$ which is not, in turn, reduced by the OEC (see Strasser 1997). In addition to the inhibition of the OEC, it has been found that the rate constants for charge separation and charge stabilization, $k_1$ and $k_2$, decrease and the rate constant for charge recombination, $k_{-1}$, increases with increasing temperature (Briantais et al. 1996). Thus, we have simulated fluorescence rise measured at high temperature using the extended RRP model and the rate constants obtained by Briantais et al. (1996) for high temperatures (see Table 1, fluorescence rise at high temperature), and by assuming inhibition of the OEC (see Theory). The result of such a simulation is shown in Fig. 3 (curve a). The simulated fluorescence signal reaches its maximal level at the time which fits very well that of FI measured with DCMU treated barley leaf at the high temperature (Fig. 2, curve d).

Using the extended RRP model, the fluorescence rise measured with DCMU treated barely leaf at room temperature can also be simulated. As for the rate constants $k_1$, $k_{-1}$, and $k_2$, we have used the values obtained by Schatz et al. (1988) and Briantais et al. (1996) for room temperature (see Table 1, fluorescence rise at room temperature). In this simulation, we have considered only the first possibility mentioned in Theory for the $P680^+$ reduction by the donor side of PSII at room temperature, i.e. $P680^+$ is reduced by $Y_Z$ which is, in turn, reduced by electrons donated from the OEC during the $S_1 \rightarrow S_2$ transition (the $S_1$ state is the only dark adapted state of the OEC). The result of the simulation is shown in Fig. 3 (curve b). Even if the fluorescence reaches its maximal level at the time which fits that of FI measured with DCMU treated barley leaf at room temperature (Fig. 2, curve c), the simulated fluorescence rise before its maximal level is quite different from the experimental one. Nevertheless, note that the minimal and the maximal values of the fluorescence intensities in both simulated curves in Fig. 3 behave in the same way as these parameters in the experimental curves (Fig. 2, curves c and d), i.e. there is an increase of the minimal fluorescence and a decrease of the maximal fluorescence at high temperatures.

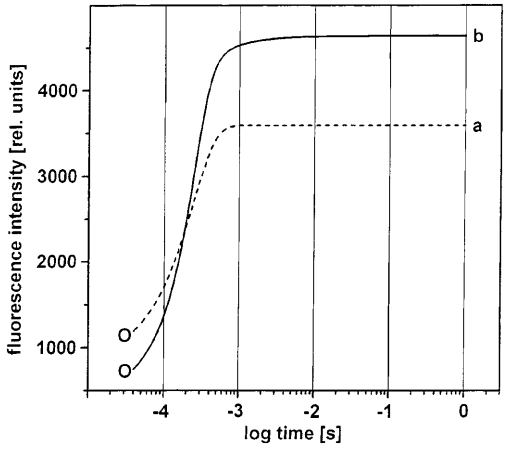


**Fig. 3** Simulations of chlorophyll *a* fluorescence rise at room and high temperatures, in relation to the function of OEC. Curve *a*: the OEC is inhibited by the high temperature and reduction of $P680^+$ occurs by $Y_Z$ which is not, in turn, reduced by the OEC (the rate constants are summarized in Table 1 (fluorescence rise at high temperature)). Curve *b*: full function of the OEC at room temperature, i.e. $P680^+$ is reduced by $Y_Z$ which is, in turn, reduced by the OEC, being all at the $S_1$ state (the rate constants are summarized in Table 1, (fluorescence rise at room temperature))

## Refinements of the simulations

Even if the maximal values of the fluorescence intensities in simulations are reached at times which fit well those of experimental courses, a closer inspection of simulated and experimental curves reveals discrepancies between them. Thus, the roles of some parameters in our simulations have been studied, first in the simulation of fluorescence rise at high temperature, and second in the simulation of fluorescence rise at room temperature. Moreover, to decide which simulation fits the experimental results best, we have plotted both the experimental and simulated FIs as the relative variable fluorescence, $rF_v$, which goes from zero to one. The $rF_v$ is defined as

$$rF_v = \frac{F(t) - F_0}{F_M - F_0}$$

where $F_M$, $F_0$, and $F(t)$ are the maximal and the minimal fluorescence intensities and fluorescence intensity at time $t$, respectively. Further, as a decrease of fluorescence after about 40 ms in Fig. 2 (curves c and d) measured with DCMU probably does not reflect photochemical reactions (DCMU treatment keeps $Q_A$ reduced at all times, ensuring a constant value of the maximal fluorescence), we have plotted all the curves only to 40 ms.

We have tested how the changes of the rate constants $k_1$, $k_{-1}$, and $k_2$ alone, caused by high temperature as reported by Briantais et al. (1996), affect the time course of the simulated fluorescence rise. Thus, we have simulated the time course of the fluorescence rise at high temperature using the same model assumption as mentioned above for this case, but the values of the rate constants $k_1$, $k_{-1}$, and $k_2$ have been those obtained for room temperature (see Table 1, fluorescence rise at room temperature). The results of this simulation is shown in Fig. 4 as curve c. The previous curve a of Fig. 3, which was simulated using the values of the rate constants $k_1$, $k_{-1}$, and $k_2$ obtained at the high temperature (see Table 1, fluorescence rise at high temperature),

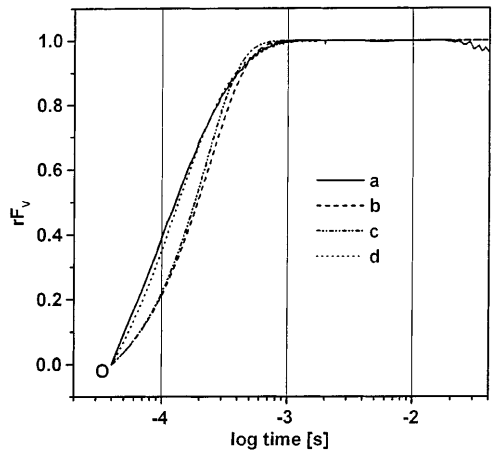


**Fig. 4** Simulated time courses of the relative variable fluorescence (*rF*v) at high temperature in relation to the values of some rate constants, and assuming the inhibition of the OEC. Curve *b*: the same as curve a in Fig. 3, i.e the OEC is inhibited and reduction of $P680^+$ occurs by $Y_Z$ which is not, in turn, reduced by the OEC (the rate constants are summarized in Table 1, fluorescence rise at high temperature). Curve *c*: the same as curve b, but the rate constants $k_1^0$, $k_{-1}^0$, $k_2^c$, $k_1^c$, $k_{-1}^c$, and $k_2^c$ are those obtained for room temperature (summarized in Table 1, fluorescence rise at room temperature). Curve d: the same as curve b, but the rate constant $k_{UU}$ is zero (i.e. no energy transfer). Curve *a* is the experimental curve d from Fig. 2 plotted by the mean of the $rF_v$

is shown as curve b in Fig. 4, and the experimental curve d of Fig. 2 is shown as curve a in Fig. 4. There is only a small difference between the courses of curves b and c, but curve b fits better the experimental curve a than curve c in the time range from about 400 μs to 1 ms. Thus, the simulation calculated with the assumption of the changes of the rate constants $k_1$, $k_{-1}$, and $k_2$ caused by the high temperature better describes the experimental results, and we conclude that changes of the rate constants at the high temperatures, as suggested by Briantais et al. (1996), really occur.

The role of the decrease of the energy transfer between the light harvesting complexes of PSII at high temperatures has been emphasized by Srivastava et al. (1997). That is why we have simulated the time course of the fluorescence rise at the high temperature using the values of the rate constant for the high temperature (see Table 1, fluorescence rise at high temperature), except for $k_{UU}$, which was zero (i.e. no energy transfer). The result of this simulation is shown in Fig. 4 (curve d). There is a less pronounced sigmoidicity of curve d in comparison with curves b and c in Fig. 4, and curve d fits almost perfectly the experimental curve a in Fig. 4. Thus, we conclude that the decrease of the energy transfer between the light harvesting complexes of PSII at high temperature, as suggested by Srivastava et al. (1997), really happens.

Curve b in Fig. 3 has been simulated, assuming that all the OEC is at the $S_1$ state (Messinger and Renger 1993) at room temperature. Nevertheless, involvement of the $S_0$ state of the OEC at room temperature after dark adaptation has also been suggested in the literature. It has been found that there are 13% of the OEC at the $S_0$ state and 87% of the OEC at the $S_1$ state (Haumann and Junge 1994) or even 25% of the OEC at the $S_0$ state and 75% of the OEC at the $S_1$ state (Kok et al. 1970) after dark adaptation. Thus, we have simulated the time course of the fluorescence rise at room temperature assuming two initial dark adapted states of the OEC, first 13% of the $S_0$ and 87% of the $S_1$, and second 25% of the $S_0$ and 75% of the $S_1$. The values of the rate constants used in these simulations were those summarized in Table 1 (fluorescence rise at room temperature), and the initial conditions were those summarized in Table 2. The results of the simulations are shown in Fig. 5, curve c (initially 13% of the $S_0$ and 87% of the $S_1$) and curve d (initially 25% of the $S_0$ and 75% of the $S_1$). The curve b of Fig. 3 (100% of the $S_1$ state) is shown as curve b in Fig. 5 and the experimental curve c of Fig. 2 is shown as curve a in Fig. 5. The simulations show clearly that the decreasing amount of the initial $S_1$ state (from 100% to 75%) leads to a better agreement of the theory with the experiment and almost perfect agreement is obtained for initially 25% of the OEC at the $S_0$ state and 75% of the OEC at the $S_1$ state. Thus, we conclude that most probably 25% of the OEC is at the $S_0$ state and 75% of the OEC at the $S_1$ state after dark adaptation, as found by Kok et al. (1970).

A global way of $P680^+$ reduction by the donor side of PSII can be also affected, in addition to the different initial states of the OEC, by the inactive OEC. Up to 30% of all the OEC has been found to be inactive at room temperature (Conjeaud et al. 1979; Schlodder et al. 1984). Thus, we have simulated the time course of the fluorescence rise

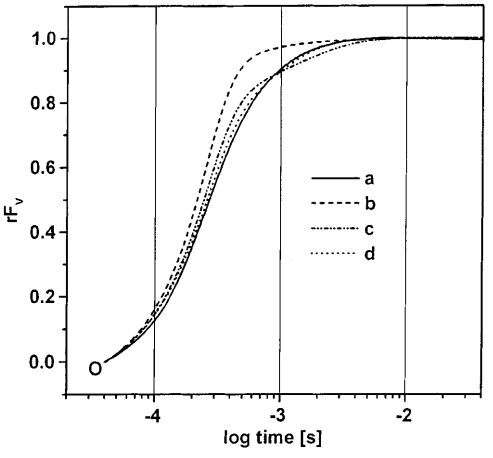


**Fig. 5** Simulated time courses of the relative variable fluorescence ($rF_v$) at room temperature in relation to the initial amounts of the $S_1$ and the $S_0$ states, and assuming full function of the OEC (the rate constants are summarized in Table 1, fluorescence rise at room temperature, and the initial conditions are summarized in Table 2). Curve *b*: the same as curve b in Fig. 3, i.e. all the OEC is initially at the $S_1$ state Curve *c*: 87% of the OEC is initially at the $S_1$ state and 13% of the OEC is initially at the $S_0$ state. Curve *d*: 75% of the OEC is initially at the $S_1$ state and 25% of the OEC is initially at the $S_0$ state. Curve *a* is the experimental curve c from Fig. 2 plotted by the mean of the $rF_v$

at room temperature assuming that 30% of all the OEC is inactive in electron donation to $Y_Z$ and the rest of the OEC (70% of all) is active. We have assumed three possibilities for the active OEC in particular simulations: first, all the active OEC is at the $S_1$ state; second, 87% of the active OEC is at the $S_1$ state and 13% of the active OEC is at the $S_0$ state; and third, 75% of the active OEC is at the $S_1$ state and 25% of the active OEC is at the $S_0$ state. The values of the rate constants used in these simulations were those summarized in Table 1 (fluorescence rise at room temperature), and the initial conditions were those summarized in Table 2. The results of the simulations are shown for the three possibilities mentioned above in Fig. 6, curves b, c, and d, respectively. The experimental curve c of Fig. 2 is shown as curve a in Fig. 6. The simulated curves show that the assumption of 30% of the inactive OEC at room temperature leads to a poor agreement of the theory with the experiment. Even the curve simulated with the assumption of 75% of the active OEC at the $S_1$ state and 25% of the active OEC at the $S_0$ state (Fig. 6, curve d), which has fitted almost perfectly the experimental curve with the assumption of no inactive OEC (Fig. 5, curve d), does not agree with the experiment (Fig. 6, curve a) now. However, the assumption of maximally 10% of the inactive OEC and 75% of the active OEC at the $S_1$ state and 25% of the active OEC at the $S_0$ state leads to a good agreement of the experimental curve with the simulated curve (data not shown). Thus, we conclude that most probably there is no or only a small amount of the inactive OEC (up to 10% of all the OEC) at room temperature.

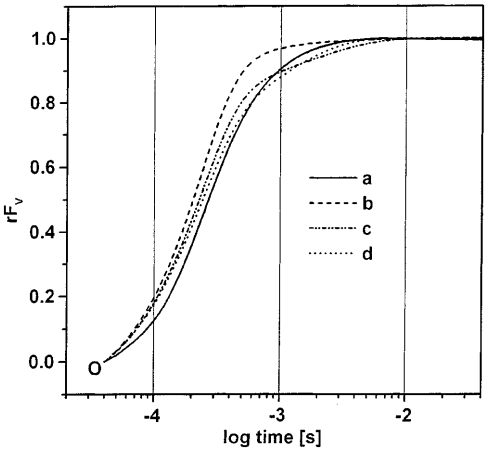


**Fig. 6** Simulated time courses of the relative variable fluorescence ($rF_v$) at room temperature in relation to the initial state of the OEC (the rate constants are summarized in Table 1, fluorescence rise at room temperature, and the initial conditions are summarized in Table 2). Curve *b*: 30% of all the OEC is inactive, and the rest 70% of the OEC is active, and initially all at the $S_1$ state. Curve *c*: 30% of all the OEC is inactive, and 87% from the rest 70% of the active OEC is initially at the $S_1$ state, and 13% from the rest 70% of the active OEC is initially at the $S_0$ state. Curve *d*: 30% of all the OEC is inactive, and 75% from the rest 70% of the active OEC is initially at the $S_1$ state, and 25% from the rest 70% of the active OEC is initially at the $S_0$ state. Curve *a* is the experimental curve c from Fig. 2 plotted by the mean of $rF_v$

## Discussion

From the results of Fig. 3 it is clear that, on the basis of the RRP model extended by a description of the function of the donor side of PSII, the fluorescence rise measured with DCMU at room and high temperatures can be well simulated and is driven by the function of the OEC. When the OEC is assumed not be inhibited, the simulated fluorescence signal reaches its maximal value at the position which fits well that of the experimental curve measured at room temperature. On the other hand, when the OEC is assumed to be inhibited, it results in reaching the maximal value of the fluorescence at the position which fits very well that of the experimental curve measured at the high temperature. If we suppose that DCMU treatment does not affect the donor side of PSII (Oettmeier and Soll 1983; Trebst and Draber 1986; Trebst 1987; Shigematsu et al. 1989), then our conclusion can be extended also to DCMU untreated plants, i.e. that the experimental fluorescence rise to the J or K step reflects the function of the OEC. When the OEC is not inhibited at room temperature, there is the J step in the FI, and when the OEC in inhibited by the high temperature, there is the K step in the FI. This conclusion supports the same suggestion of Guissé et al. (1995a, b), Srivastava et al. (1997), and Strasser (1997).

However, when, in addition to the inhibition of the OEC, the rate constant for energy transfer between the closed and the open RCII, $k_{UU}$, is assumed to be zero, the simulated curve (Fig. 4, curve d) better describes the experimental fluorescence rise measured with DCMU at the high temperature (Fig. 4, curve a). This is in agreement with the results of Srivastava et al. (1997) who have suggested that changes in the organization of the light harvesting complexes of PSII occur at high temperatures. On the other hand, the course of the curve which simulates the fluorescence rise with the DCMU at room temperature is affected by demands for the initial state of the OEC. The simulated curve describes best the experimental course of the fluorescence rise measured with DCMU at room temperature (Fig. 5, curve a), when 75% of the OEC is at the $S_1$ state and 25% of the OEC is at the $S_0$ state (Fig. 5, curve d). This result supports the suggestion of 75% of the OEC at the $S_1$ and 25% of the OEC at the $S_0$ state found for the dark adapted state by Kok et al. (1970). Further, the assumption of 30% of the inactive OEC in dark adapted state at room temperature suggested by Conjeaud et al. (1979) and Schlodder et al. (1984) does not lead to a better agreement of the simulations with the experiments (Fig. 6).

The roles of other parameters at the extended RRP model which have not been studied by us can also be discussed. Different values of the rate constants $k_S$, describing the transition from the $S_i$ state of the OEC to the $S_{i+1}$ state of the OEC, have been reported in the literature. The $k_S$ for the $S_1 \rightarrow S_2$ transition has been

determined in a relatively narrow interval, 7140–33330 $s^{-1}$ (see Rappaport et al. 1994), but two extreme values of the $k_S$ for the $S_0 \rightarrow S_1$ transition have been found: 4000 $s^{-1}$ (Rappaport et al. 1994) and $3.33 \times 10^5$ $s^{-1}$ (van Leeuwen et al. 1993). We have chosen the values of 10000 $s^{-1}$ (for the $S_1 \rightarrow S_2$ transition) and 5000 $s^{-1}$ (for the $S_0 \rightarrow S_1$ transition) which lie in the intervals mentioned above. However, it is clear that usage of the extreme values of the $k_S$ would lead to a change of the course of the simulated fluorescence rise. It is also possible that a change of the light gradient across the leaf can occur during the high temperature treatment. Such a change would probably affect the rate of exciton formation, $k_L$, which, of course, would lead to a change of the course of the simulated fluorescence rise. The lack of experimental results dealing with this topic has not enabled us to use this effect in our simulations. A consideration of different types of PSII heterogeneity would also affect the course of the simulated fluorescence rise (mainly PSII antenna heterogeneity). An effect of the PSII antenna heterogeneity, but without consideration of the function of the donor side of PSII, on the course of fluorescence rise with DCMU at room temperature has been studied extensively by Lavergne and Trissl (1995), Trissl and Lavergne (1995), and Vavilin et al. (1998). Even if the authors have obtained almost perfect agreement of the theory with the experiment, our results clearly show that the fluorescence rise can be well simulated when the RRP model is extended by a description of the function of the donor side of PSII, without the assumption of the PSII antenna heterogeneity. Nevertheless, more research is necessary to find a complete theory of the fluorescence rise.

**Acknowledgements** This work was done in the laboratory of the Division of Biophysics, Department of Experimental Physics, Faculty of Science, Palacký University, Olomouc, Czech Republic. We would like to thank Docent Jan Nauš, the head of the laboratory, for the possibility to do this work in the laboratory.

## References

Baake E, Schlöder JP (1992) Modelling the fast fluorescence rise of photosynthesis. Bull Math Biol 54: 999–1021

Barthélemy X, Popovic R, Franck F (1997) Studies on the O-J-I-P transient of chlorophyll fluorescence in relation to photosystem II assembly and heterogeneity in plastids of greening barley. J Photochem Photobiol B39: 213–218

Breton J (1983) The emission of chlorophyll in vivo. Antenna fluorescence or ultrafast luminescence from reaction center pigments. FEBS Lett 159: 1–5

Brettel K, Schlodder E, Witt HT (1984) Nanosecond reduction kinetics of photoxidized chlorophyll-$a_{II}$ (P-680) in single flashes as a probe for the electron pathway, H-release and charge accumulation in the $O_2$-evolving complex. Biochim Biophys Acta 766: 403–415

Briantais J-M, Dascosta J, Goulas Y, Ducruet J-M, Moya I (1996) Heat stress induces in leaves an increase of the minimum level of chlorophyll fluorescence, $F_0$: a time-resolved analysis. Photosynth Res 48: 189–196

Britt RD (1996) Oxygen evolution. In: Ort DR, Yocum CF (eds) Oxygenic photosynthesis: the light reactions. Kluwer, Dordrecht, pp 137–164

Bruce D, Samson G, Carpenter C (1997) The origins of nonphotochemical quenching of chlorophyll fluorescence in photosynthesis. Direct quenching by $P680^+$ in photosystem II enriched membranes at low pH. Biochemistry 36: 749–755

Butler WL (1972) On the primary nature of fluorescence yield changes associated with photosynthesis. Proc Natl Acad Sci USA 69: 3420–3422

Conjeaud H, Mathis P, Paillotin G (1979) Primary and secondary electron donors in photosystem II of chloroplasts. Rates of electron transfer and location in the membrane. Biochim Biophys Acta 546: 280–291

Cramer WA, Whitmarsh J, Low PS (1981) Differential scanning calorimetry of chloroplast membranes: identification of an endothermic transition associated with the water-splitting complex of photosystem II. Biochemistry 20: 157–162

Dau H (1994) Molecular mechanism and quantitative models of variable photosystem II fluorescence. Photochem Photobiol 60: 1–23

Debus RJ (1992) The manganese and the calcium ions of photosynthetic oxygen evolution. Biochim Biophys Acta 1102: 269–352

Delosme R (1967) Etude de l'induction de fluorescence des algues vertes et des chloroplastes au début d'une illumination intense. Biochim Biophys Acta 143: 108–128

Govindjee (1995) Sixty-three years since Kautsky: chlorophyll *a* fluorescence. Aust J Plant Physiol 22: 131–160

van Grondelle R (1985) Excitation energy transfer, trapping and annihilation in photosynthetic systems. Biochim Biophys Acta 811: 147–195

Guissé B, Srivastava A, Strasser RJ (1995a) Effects of high temperature and water stress on the polyphasic chlorophyll *a* fluorescence transient of potato leaves. In: Mathis P (ed) Photosynthesis: from light to biosphere, vol IV. Kluwer, Dordrecht, pp 913–916

Guissé B, Srivastava A, Strasser RJ (1995b) The polyphasic rice of the chlorophyll *a* fluorescence (O-K-J-I-P) in heat-stressed leaves. Arch Sci Genéve 48: 147–160

Hansson Ö, Wydrzynski T (1990) Current perceptions of photosystem II. Photosynth Res 23: 131–162

Haumann M, Junge W (1994) Extent and rate of proton release by photosynthetic water oxidation in thylakoids: electrostatic relaxation versus chemical production. Biochemistry 33: 864–872

Kautsky H, Hirsch A (1931) Neue Versuche zur Kohlensäureassimilation. Naturwissenschaften 19: 964

Kok B, Forbush B, McGloin M (1970) Cooperation of charges in photosynthetic $O_2$ evolution – I. A linear four step mechanism. Photochem Photobiol 11: 457–475

Krause GH, Weis E (1991) Chlorophyll fluorescence and photosynthesis: the basis. Annu Rev Plant Physiol Plant Mol Biol 42: 313–349

Laible PD, Zipfel W, Owens TG (1994) Excited state dynamics in chlorophyll-based antennae: The role of transfer equilibrium. Biophys J 66: 844–860

Lavergne J, Trissl H-W (1995) Theory of fluorescence induction of photosystem II: derivation of analytical expressions in a model including exciton-radical-pair equilibrium and restricted energy transfer between photosynthetic units. Biophys J 68: 2474–2492

Lazár D (1999) Chlorophyll *a* fluorescence induction. Biochim Biophys Acta 1412: 1–28

Lazár D, Ilík P (1997) High-temperature induced chlorophyll fluorescence changes in barley leaves. Comparison of the critical temperatures determined from fluorescence induction and from fluorescence temperature curve. Plant Sci 124: 159–164

Lazár D, Nauš J, Matoušková M, Flašarová M (1997a) Mathematical modeling of changes in chlorophyll fluorescence induction caused by herbicides. Pestic Biochem Physiol 57: 200–210

Lazár D, Ilík P, Nauš J (1997b) An appearance of K-peak in fluorescence induction depends on the acclimation of barley leaves to higher temperatures. J Lumin 72–74: 595–596

Lazár D, Brokeš M, Nauš J, Dvořák L (1998) Mathematical modelling of 3-(3′,4′-dichlorophenyl)-1,1-dimethylurea action in plant leaves. J Theor Biol 191: 79–86

van Leeuwen P, Heimann C, Gast P, Dekker JP, van Gorkom HJ (1993) Flash-induced redox changes in oxygen-evolving spinach photosystem II core particles. Photosynth Res 38: 169–176

Lichtenthaler HK (1987) Chlorophyll and carotenoids: pigments of photosynthetic biomembranes. Methods Enzymol 148: 350–382

Masamoto K, Nishimura M (1978) Effects of ethanol on the interaction of photosynthetic processes in spinach chloroplasts. Plant Cell Physiol 19: 1543–1552

Melis A (1996) Excitation energy transfer: functional and dynamic aspects of *Lhc* (*cab*) proteins. In: Ort DR, Yocum CF (eds) Oxygenic photosynthesis: the light reactions. Kluwer, Dordrecht, pp 523–538

Messinger J, Renger G (1993) Generation, oxidation by the oxidized form of the tyrosine of polypeptide D2, and possible electronic configuration of the redox states $S_0$, $S_{-1}$ and $S_{-2}$ of the water oxidase in isolated spinach thylakoids. Biochemistry 32: 9379–9386

Neubauer C, Schreiber U (1987) The polyphasic rice of chlorophyll fluorescence upon onset of strong continuous illumination: I. Saturation characteristics and partial control by the photosystem II acceptor side. Z Naturforsch 42c: 1246–1254

Oettmeier W, Soll HJ (1983) Competition between plastoquinone and 3-(3,4-dichlorophenyl)-1,1-dimethylurea at the acceptor side of photosystem II. Biochim Biophys Acta 724: 287–297

Owens TG (1996) Processing of excitation energy by antenna pigments. In: Baker NR (ed) Photosynthesis and the environment. Kluwer, Dordrecht, pp 1–23

Pfündel E (1998) Estimating the contribution of photosystem I to total leaf chlorophyll fluorescence. Photosynth Res 56: 185–195

Rappaport F, Blanchard-Desce M, Lavergne J (1994) Kinetics of electron transfer and electrochromic change during the redox transitions of the photosynthetic oxygen-evolving complex. Biochim Biophys Acta 1184: 178–192

Reifarth F, Curislen G, Renger G (1997) Fluorometric equipment for monitoring $P680^+$ reduction in PSII preparations and green leaves. Photosynth Res 51: 231–242

Schatz GH, Brock H, Holzwarth AR (1988) Kinetic and energetic model for the primary processes in photosystem II. Biophys J 54: 397–405

Schlodder E, Brettel K, Witt HT (1984) Analysis of the Chl-$a_{II}^-$ reduction kinetics with nanosecond time resolution in oxygen-evolving photosystem II particles from *Synechococcus* at 680 and 824 nm. Biochim Biophys Acta 765: 178–185

Schreiber U, Neubauer C (1987) The polyphasic rice of chlorophyll fluorescence upon onset of strong continuous illumination: II. Partial control by the photosystem II donor side and possible ways of interpretation. Z Naturforsch 42c: 1255–1264

Shigematsu Y, Satoh F, Yamada Y (1989) A binding model for phenylurea herbicides based on analysis of a Thr 264 mutation in D-1 protein of tabacco. Pestic Biochem Physiol 35: 33–41

Shrinkarev VP, Govindjee (1993) Insight into the relationship of chlorophyll *a* fluorescence yield to the concentration of its natural quenchers in oxygenic photosynthesis. Proc Natl Acad Sci USA 90: 7466–7469

Sonneveld A, Rademaker H, Duysens LNM (1979) Chlorophyll *a* fluorescence as a monitor of nanosecond reduction of the photooxidized primary donor $P\text{-}680^+$ of photosystem II. Biochim Biophys Acta 548: 536–551

Srivastava A, Guissé B, Greppin H, Strasser RJ (1997) Regulation of antenna structure and electron transport in photosystem II of *Pisum sativum* under elevated temperature probed by the fast polyphasic chlorophyll *a* fluorescence transient: OKJIP. Biochim Biophys Acta1320: 95–106

Stirbet A, Strasser RJ (1995) Numerical simulation of the fluorescence induction in plants. Arch Sci Genèva 48: 41–60

Stirbet A, Govindjee, Strasser BJ, Strasser RJ (1995) Numerical simulation chlorophyll *a* fluorescence induction in plants. In: Mathis P (ed) Photosynthesis: from light to biosphere, vol II. Kluwer, Dordrecht, pp 912–922

Stirbet A, Govindjee, Strasser BJ, Strasser RJ (1998) Chlorophyll *a* fluorescence induction in higher plants: modelling and numerical simulation. J Theor Biol 193: 131–151

Strasser BJ (1997) Donor side capacity of photosystem II probed by chlorophyll *a* fluorescence transients. Photosynth Res 52: 147–155

Strasser RJ, Govindjee (1991) The $F_0$ and the O-J-I-P fluorescence rise in higher plants and algae. In: Argyroudi-Akoyunoglou JH (ed) Regulation of chloroplast biogenesis. Plenum Press, New York, pp 423–426

Strasser RJ, Govindjee (1992) On the O-J-I-P fluorescence transient in leaves and DI mutants of *Chlamydomonas reinhardtii*. In: Murata M (ed) Research in photosynthesis, vol 2. Kluwer, Dordrecht, pp 29–32

Strasser RJ, Srivastava A, Govindjee (1995) Polyphasic Chlorophyll *a* fluorescence transient in plants and cyanobacteria. Photochem Photobiol 61: 32–42

Thompson LK, Sturtevant JM, Brudvig GW (1986) Differential scanning calorimetric studies of photosystem II: evidence for a structural role for cytochrome $b_{599}$ in the oxygen-evolving complex. Biochemistry 25: 6161–6169

Tresbst A (1987) The three-dimensional structure of the herbicide binding niche on the reaction centre polypeptides of photosystem II. Z Naturforsch 42c: 742–750

Tresbst A, Draber W (1986) Inhibitors of photosystem II and the topology of the herbicide and $Q_B$ binding polypeptide in the thylakoid membrane. Photosynth Res 10: 381–392

Trissl H-W, Lavergne J (1995) Fluorescence induction from photosystem II: analytical equations for the yields of photochemistry and fluorescence derived from analysis of a model including exciton-radical pair equilibrium and restricted energy transfer between photosynthetic units. Aust J Plant Physiol 22: 183–193

Trissl H-W, Gao Y, Wulf K (1993) Theoretical fluorescence induction curves derived from coupled differential equations describing the primary photochemistry of photosystem II by an exciton-radical pair equilibrium. Biophys J 64: 974–988

Vavilin DV, Tyystjärvi E, Aro E-M (1998) Model for the fluorescence induction curve of photoinhibited thylakoids. Biophys J 75: 503–512